Report

Behavioral Analysis of Cuttlefish Traveling Waves and Its Implications for Neural Control

Andres Laan,[1] Tamar Gutnick,[1] Michael J. Kuba,[1] and Gilles Laurent[1,*]
[1]Department of Neural Systems and Coding, Max Planck Institute for Brain Research, Max-von-Laue Strasse 4, 60438 Frankfurt, Germany

Summary

Traveling waves (from action potential propagation to swimming body motions or intestinal peristalsis) are ubiquitous phenomena in biological systems and yet are diverse in form, function, and mechanism. An interesting such phenomenon occurs in cephalopod skin, in the form of moving pigmentation patterns called "passing clouds" [1]. These dynamic pigmentation patterns result from the coordinated activation of large chromatophore arrays [2]. Here, we introduce a new model system for the study of passing clouds, *Metasepia tullbergi*, in which wave displays are very frequent and thus amenable to laboratory investigations. The mantle of *Metasepia* contains four main regions of wave travel, each supporting a different propagation direction. The four regions are not always active simultaneously, but those that are show synchronized activity and maintain a constant wavelength and a period-independent duty cycle, despite a large range of possible periods (from 1.5 s to 10 s). The wave patterns can be superposed on a variety of other ongoing textural and chromatic patterns of the skin. Finally, a traveling wave can even disappear transiently and reappear in a different position ("blink"), revealing ongoing but invisible propagation. Our findings provide useful clues about classes of likely mechanisms for the generation and propagation of these traveling waves. They rule out wave propagation mechanisms based on delayed excitation from a pacemaker [3] but are consistent with two other alternatives, such as coupled arrays of central pattern generators [3] and dynamic attractors on a network with circular topology [4].

Results

Soft-bodied cephalopod skin is covered with hundreds to millions of elastic pigmented cells called chromatophores, whose size can be rapidly and individually altered by neural activation of radial muscles [1]. Coordinated size changes across arrays of chromatophores are necessary to generate the large variety of visual displays observed in squid, cuttlefish, and octopus [2]. One such display is the "passing cloud," a dark band that travels across the body of the animal [1]. The tropical cuttlefish *Metasepia tullbergi* (Appellof, 1886) proved to be an excellent model organism to study these traveling waves due to the animal's small size, the high occurrence of wave displays, and the slow speed of the animal (convenient for filming). A keeping permit was obtained by the Veterinary Department of the city of Frankfurt according to section 11 of the German Animal Welfare Act.

*Correspondence: gilles.laurent@brain.mpg.de

CrossMark

Four Main Regions of Wave Travel

We filmed five adult, freely behaving *M. tullbergi* in their home tank from above at a rate of 50 frames per second (fps) at high-definition (HD) resolution. Based on the observed wave displays (Movie S1 available online), the left half and right half of the body of *M. tullbergi* can each be divided into four regions (Figures 1A and 1B, regions 1–4). The regions are bilaterally symmetric, and each region supports a distinct traveling wave with a unique region-specific direction of travel (Figure 1A, arrows). The waves do not cross region boundaries. Within a region, the direction of travel is constant over time and across animals, although the travel velocity varies within each animal (Figures 1C and 1D). In each region, the wave always appears as a pigmented moving band with steeply fading boundaries. The wavelength of the display (see details below) is approximately commensurate with the total length of travel. Hence, each region usually supports only one pigmented moving band, except when that band approaches the distal edge of its region of travel; at that time, a second band appears at the proximal edge.

The wave in the anterior region (Figure 1A, regions 1 and 1′) emerges at the anterior rim of the mantle and travels posteriorly. When it occurs bilaterally, the anterior wave forms a single, continuous, jagged, C-shaped band extending from one fin line to the other, on each side of the animal (Figure 1A, green zone). The medial arc of this band travels on the mediodorsal mantle (region 1′), where it eventually collides with the boundary of region 3 and disappears. The disappearance of the medial arc of the anterior wave breaks the band into two isolated lateral bands, one on each side of the animal; each band continues traveling until it reaches the region 2 boundary and vanishes.

The body of *M. tullbergi* has a relatively smooth mediodorsal surface, separated from its downward sloping laterodorsal surfaces by two longitudinal ridges of papillae (one on each side of the animal; Figures 1A and 1B). A second zone of wave initiation is located slightly lateral to this ridge (Figure 1A, cyan bands). From there and on each side of the body, two waves begin their propagation simultaneously: one travels laterally toward the fin line (region 2) while the other propagates medially (region 3) toward the dorsal midline. Propagation in region 2 ends when the wave reaches the fin line. In region 3, the centripetal waves on each side of the body collide at the midline.

The last region of wave propagation (Figure 1A, region 4) is located in the posterior half of the mantle, with the initiation point at the tip (Figure 1A, red). From there, a right-side band and left-side band simultaneously begin to move anteriorly toward the head. The left and right bands meet at the midline, thus forming a traveling V shape. As observed with the anterior C-shaped band, the V breaks into two separate bands when its apex collides with the posterior boundary of region 3 (Figure 1B).

Superposition of Wave and Static Patterns

Coleoid cephalopods use their chromatophore system for a variety of cryptic and social displays. The camouflage displays in particular are static, multiform, and highly adaptive [1, 2]. We
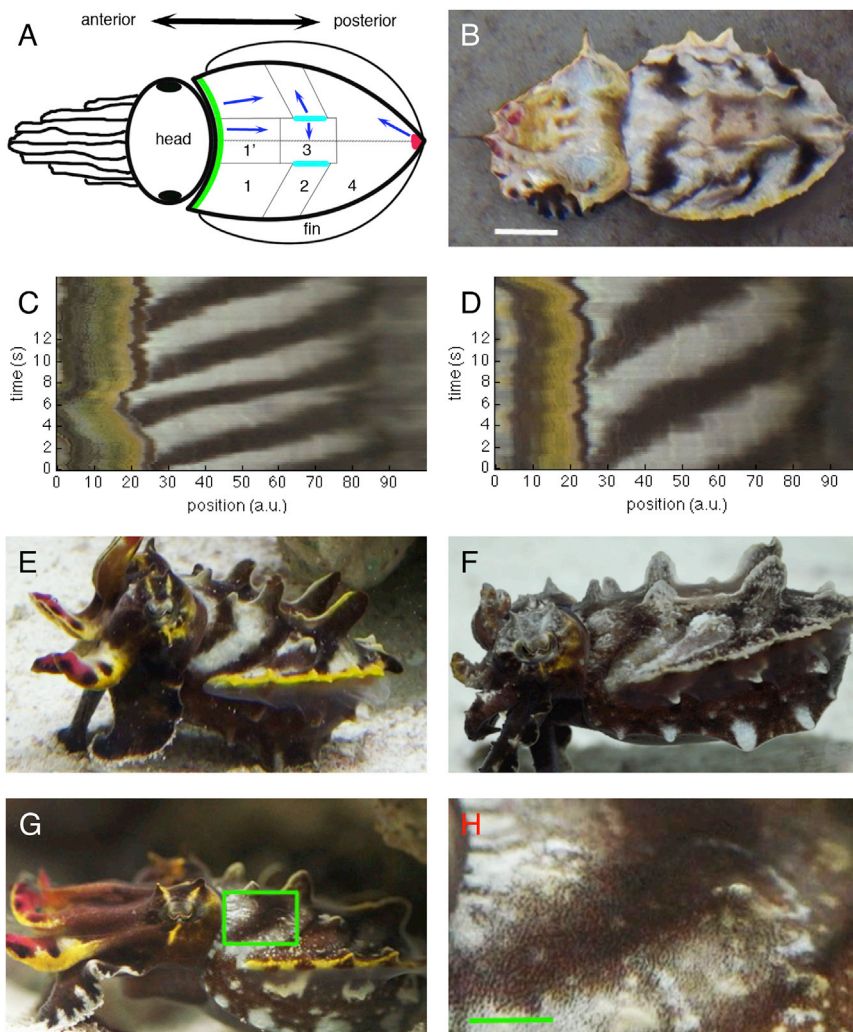
Figure 1. Multiple Regions of Wave Travel

(A) Schematic of the animal with depiction of the four regions of wave travel on the dorsal mantle. The regions and wave displays are almost always bilaterally symmetric. Regions of wave travel (with boundaries as thin lines) are indicated on left side of the animal; direction of travel within each region is denoted by arrow on right side. Each region supports only one direction of travel, and waves do not cross region boundaries. The green line marks the mantle rim wave initiation zone; the cyan line indicates the middle wave initiation zone; the crimson spot indicates the third wave initiation zone at the mantle tip. Region names are as used in text: 1 indicates anterior, 1′ indicates anterior dorsal, 2 indicates middle, 3 indicates central, and 4 indicates posterior.

(B) Still video image of one of the experimental animals during wave display. Intensity of background is reduced, and contrast of the animal is enhanced to improve visibility. Scale bar represents 1cm.

(C and D) Time position intensity plots for two wave displays with two different wave propagation velocities (fast in C, slow in D). Each column depicts the pigmentation of a one-pixel-wide parasagittal strip in region 1 of the animal's body over time (sampling rate is 5 Hz); rows show the same strip along the body of the animal at successive times. Motion thus appears as diagonal lines, whereas static patterns form vertical columns. Jaggedness is due to superimposed motion of the animal or contractions of the mantle.

(E–H) Single video frames of animals expressing traveling waves on four different static body backgrounds: flamboyant (E); mottle (F); flamboyant-mottle (G). Images are contrast enhanced to improve visibility. Box in (G) indicates position of expanded view in (H). Note the pigmented dots, corresponding to single chromatophores. Green scale bar of (H) represents 2 mm.

observed that the traveling waves can be superimposed on a wide variety of static body patterns (e.g., flamboyant or mottle) and textures, which are also produced by activity in the chromatophore system and skin musculature (Figures 1E–1H). Overall, we observed that *M. tullbergi* can express wave displays in behavioral contexts as diverse as hunting, swimming, walking, mating, resting under rocks, threat posturing, and egg maintenance. The waves ceased to be visible mainly during maintained periods of quiescence (tens of minutes to hours).

Wavelength, Period, Duty Cycle, and Velocity

For quantitative analysis, we filmed *M. tullbergi* with a high-speed camera (100 fps) at HD resolution from a lateral view. Each video lasted 19 s. We analyzed the temporal features of the wave in region 1 because it is the largest and most conspicuous of the four regions when observed from a lateral view. Within this region, we selected an easily identifiable skin element, which we call "patch" (see Supplemental Experimental Procedures and Figure S1A), on the animals' bodies (different for each individual, function of filming angle, textural and pattern states of the animal), and the temporal characteristics of the wave were studied using visual annotation.

Within the patch, we documented the following parameters: time of darkening onset (t_0) (i.e., chromatophore expansion; see Figure S1); time of return to baseline intensity (t_1); time of onset of the following wave of chromatophore expansion (t_2). We then calculated the cycle period (T; $T = t_2 - t_0$), its variability, and the duty cycle (C; $C = [t_1 - t_0]/T$). Over a sample of 98 cycles pooled across 28 instances and 5 animals, we found the period to vary between 1.5 s and 10 s, i.e., a 6-fold variation (Figure 2A; Supplemental Experimental Procedures). A similar range was observed within individual animals (Figure 2B). Despite this wide variation, the duty cycle was 0.45 ± 0.096 and independent of the period (Figures 2A and 2B; $R^2 = 0.025$; 95% confidence intervals, 0.17–0.22; Fisher's z transformation was used for calculation of all correlation coefficient confidence intervals). We next measured the wavelength (distance between two successive pigmentation band centers) of the moving pattern in region 1 and its ratio to the maximum distance between anterior and posterior region boundaries (ratio of green to yellow lines, "wavelength fraction"; Figure 2C). Again, this ratio did not depend on the period (Figure 2D; $R^2 = 0.071$; 95% confidence intervals, 0.29–0.414; n = 31 cycles). In conclusion, the pattern within region 1 consisted of a succession of moving bands separated by a constant distance (the wavelength) that was smaller (by about 30%) than the total region of travel. Although the width of each pigmented band (duty cycle) varies, it varies independently of the period (and velocity). Finally, because the period varies about 6-fold while the wavelength is constant, the
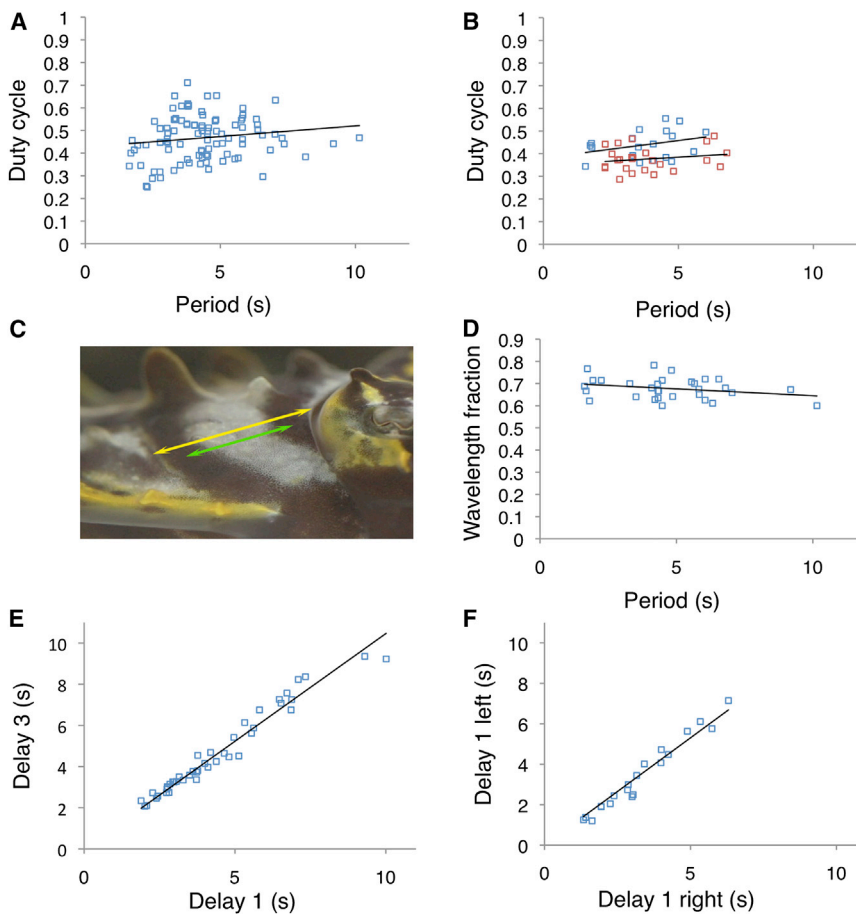
Figure 2. Duty Cycle, Wavelength, and Interregion Synchrony Are Independent of the Period

(A) Duty cycle versus period (n = 100 cycles; data pooled across five animals). The period is variable by a factor of 6, from 1.6 s to 10 s, yet the duty cycle is period independent. For details on linear regression, see Results.

(B) Duty cycle versus period for one male (blue; n = 19 cycles) and one female (red; n = 28 cycles) animal, illustrating period variability within individual animals.

(C) Definition of wavelength fraction: yellow arrow depicts length of travel region; green arrow shows wavelength (the distance between the centers of the two traveling bands; see Supplemental Experimental Procedures). Wavelength fraction is calculated as the ratio of wavelength to travel region length.

(D) Graph of wavelength fraction versus period (n = 31 cycles).

(E) Synchronization of regions 1 (anterior) and 4 (posterior), indicated by the strong correlation between anterior and posterior delays (for definition, see Results).

(F) Synchronization of regions 1 on opposite sides of the body, as in (E) (see Supplemental Experimental Procedures for definition of reference points).

propagation velocity also varies 6-fold. Two examples of velocities can be seen (as the slopes of the dark band position over time) in Figures 1C and 1D.

Coordination across Regions

We next investigated whether the wave patterns expressed in different regions of the body are synchronized. In videos where both the posterior boundary of region 1 and the anterior boundary of region 4 (i.e., each boundary formed with region 2) were clearly visible, we measured the arrival times of the anterior wave at the border between regions 1 and 2 for successive waves (times u^a_1 and u^a_2) and the arrival time of the posterior wave (u^p_1) at the border between regions 4 and 2, which was closest in time to u^a_2. Plotting the anterior versus posterior delay ([$u^a_2 - u^a_1$] versus [$u^a_2 - u^p_1$]; Figure 2E) revealed a very strong correlation (R^2 = 0.96; 95% confidence intervals, 0.93–0.98; n = 50 cycles; see Supplemental Experimental Procedures) between the two measures. Because the posterior delay was determined relative to events in region 1, this result is possible only if the anterior and posterior waves remain synchronous despite variations in period. A similar analysis between regions 1 on opposite sides (Figure 2F) and between anterior and middle regions on one side (Figure S1B) confirmed this result. Hence, when waves occur on several regions simultaneously, they are perfectly synchronized.

Selective Spatial Gating of the Wave

The synchrony found among the eight body regions is remarkable not only because the directions of wave travel differ across regions (Figure 1A) but also because traveling-wave expression can be gated locally. Whereas regions 1 and 4 always appeared to be coactive, waves in these regions often occurred without corresponding activity in regions 2 or 3 (Movie S1). The animals remained sufficiently still for automated analysis in 16 out of 88 high-speed recordings. In each recording, we selected two small patches of skin (Figure 3A, region 1 [blue] and region 2 [red]) and measured the intensity of each as functions of time (see also Supplemental Experimental Procedures). Two typical examples are shown in Figures 3B and 3C. We cross-correlated the intensity profiles in regions 1 and 2 and measured the maximum absolute value of the Pearson cross-correlation within a 4 s window, and we observed that those values formed two well-separated clusters (Figure 3D, y axis). We independently visually classified the same videos into two categories: category a contained displays in which both region 1 and region 2 visibly supported a wave, and category b contained displays in which only region 1 showed wave activity. The plot of visual classification against correlation (Figure 3D) revealed perfect agreement. Using the thus-validated visual annotation in videos where automated analysis proved impossible due to motion of the animal, we found that 25% (22 out of 88) of our recordings contained an inactive middle region.

High-speed recordings focused mainly on a lateral view of the animals. To better study the control of wave expression across regions, we filmed HD recordings at 50 fps from above, enabling filming from the dorsal side and thus revealing all four regions on both sides of the animal. Following the animals in this manner over a period of 5 days (~2 hr of footage; ~1,600 wave activity cycles), we documented the prevalence of coordinated wave patterns. We used the notation 1/.../4 to denote a pattern where regions between 1 and 4 on one side supported a wave (e.g., 1/3/4 means that regions
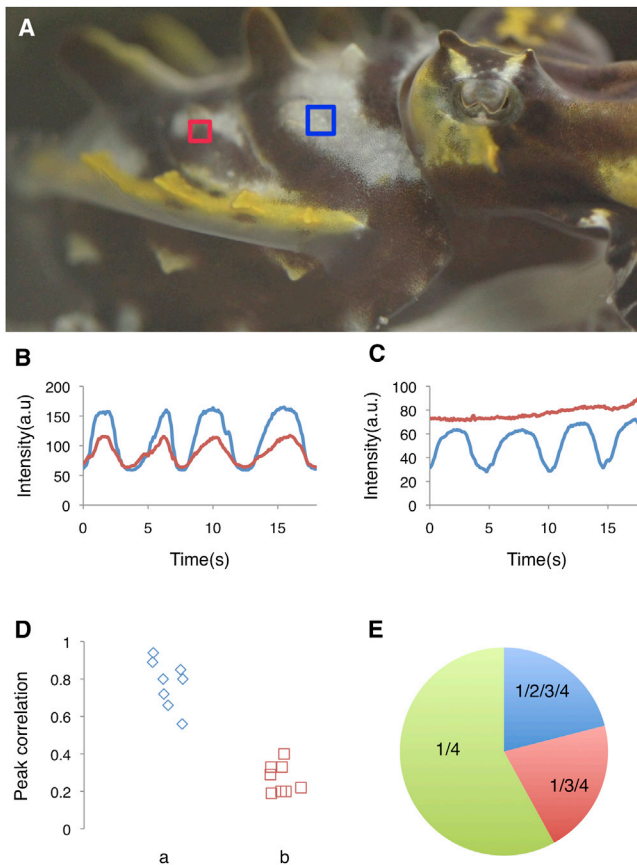
Figure 3. Wave Coordination across Regions

(A) Analysis regions (blue indicates region 1; red indicates region 2) from which intensity variations during a wave display were calculated in (B)–(D).
(B) Plot of region intensity variations for case where regions 1 and 2 both support a traveling wave. Note the correlation.
(C) Plot of region intensity variations for case where only region 1 supports a traveling wave.
(D) Peak cross-correlation values between the signals of regions 1 and 2 for visually classified categories a and b. Category a: regions 1 and 2 both support a traveling wave as per visual inspection. Category b: only region 1 supports a traveling wave. Note the agreement between automated and visual categorizations.
(E) Pie chart showing the relative abundance of the three observed types of coordinated activity patterns.

1, 3, and 4, but not region 2, supported a wave). Out of all possible pattern combinations, we observed only patterns 1/4 (58%), 1/3/4 (21%), and 1/2/3/4 (21%) (% = percentage of total observation time). Patterns such as 1/3 or 2/4 were never observed. The wave displays mentioned above were all symmetrical, except for a single 40 s observation of an asymmetric wave display.

In two out of five animals (both females), we observed a previously unreported phenomenon, which we call "blink". A blink is a transient (about 0.5 s) and local (within a region) reduction of the intensity of the traveling wave (Figure 4A; Movie S1). Blinks did not greatly affect wave propagation, even though wave pigmentation intensity could be so reduced as to mask the traveling band entirely (in 26% out of a total of n = 40 blinks). If two pigmented bands were visible in the same region (e.g., at the anterior and posterior boundaries of region 1) at the moment of blink initiation, both bands underwent a simultaneous reduction in amplitude. Anecdotally, blinks coincided

with the transient appearance of a dark line on the third tentacle and a twitch of the upper region of the tentacles.

We quantified the effect of blinks on wave propagation by measuring the travel fraction. If a particle travels at constant velocity the length L of a track in time τ, then in time t, it travels $l = L \times t/\tau$. If velocity is constant, the travel fraction (l/L over t/τ) equals one. Analysis of 35 control passing clouds (1 s long analysis windows) indeed found the travel fraction to be quite close to one (1.04 ± 0.1, p = 0.01, significantly different from 1, two-tailed t test). With 40 passing clouds interrupted by blinks, the travel fraction was very slightly but significantly reduced to 0.93 ± 0.18 (p = 0.001, significantly different from control, two-tailed t test). Thus, blinks appear to have only very moderate effects on passing-cloud propagation. Possible alternative outcomes (e.g., interruption followed by resumption: expected travel fraction is 0.52 because the average blink lasts 0.48 s; obliteration: expected travel fraction is 0.25 because blinks begin on average 12 frames after the start of the 50 frame analysis window) were never observed. Blinks did not represent damage to a local patch of chromatophores because animals that displayed blinks also displayed typical uninterrupted passing clouds interspersed between blinks, and blink initiation position (marked as the location of the dark moving band at the beginning of its intensity reduction) tiled the entire zone of propagation (Figure 4B).

Discussion

Descriptions of cephalopod passing clouds (with the exception of *Octopus cyanea* [5]) have been side notes in field or laboratory observations of camouflage, hunting, or mating behavior in *Sepia officinalis* [6, 7] or *Sepia apama* [8]. In these species, the expression of passing clouds is sporadic, making laboratory studies difficult. By contrast, the nearly continuous expression of passing clouds in *M. tullbergi* (and possibly related species *Metasepia pfefferi* [9]) should greatly facilitate controlled and quantitative investigations of their underlying causes.

Our descriptive analysis of passing clouds provides some hints as to what these underlying mechanisms might and might not be. First, because the waves propagate at a wide range of velocities (approximately 6-fold), they are unlikely to be due to simple diffusive processes such as calcium diffusion in the mantle. Second, we observed that passing clouds propagate even when large fields of chromatophores remain silent in part of the wave's propagation zone (blinks). This motion, through inactive fields, rules out the role of direct interchromatophore-muscle coupling [10, 11] in wave propagation. Electrical or mechanical coupling between chromatophore muscles has been suggested to underlie the propagation of a different wave-like pattern, observed in denervated or postmortem cephalopod skin and known as "wandering clouds" [1, 12–14]. At least two observations made in our paper indicate that passing clouds and wandering clouds are mechanistically distinct. First, wandering clouds travel in all possible directions in the skin, and their propagation velocity is about ten times slower ([12]; A.L., T.G., M.J.K., and G.L., unpublished data in *S. officinalis*). Second, myogenic propagation is incompatible with our observation that the pattern's wavelength is constant while the period is variable (see discussion on classes of pattern-generating mechanisms below).

Collectively, our results on passing clouds argue for central rather than peripheral wave generation and hence are in favor of circuit mechanisms originating with or proximal to the
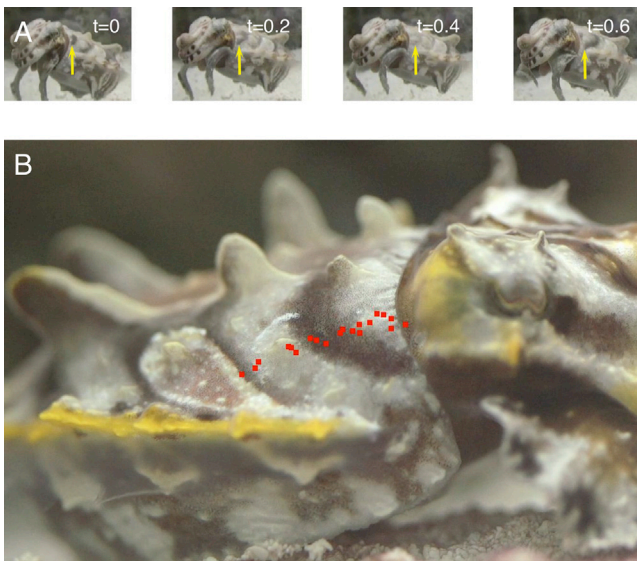
Figure 4. Blinks

(A) Time-lapse illustration of a blink. The multipanel image shows selected video frames (t in seconds), illustrating the transient and nearly complete disappearance of the dark band (yellow arrows) in the third panel and its reappearance at a new position in the fourth panel.

(B) Blink positions (red dots; n = 20) tile the region of wave travel. A red dot was placed on the animal's body to mark the position of the leading edge of the traveling pigmented band at the beginning of a blink. Each dot represents a different blink. This shows that blinks can be initiated at any moment of wave propagation.

chromatophore motoneuron populations. Because these motoneurons lie in the chromatophore lobes [15], those circuits should first be sought within that region. Because the passing clouds can be superposed on a variety of static displays (i.e., on a variety of chromatophore relaxation states), it seems unlikely that the motoneurons themselves form or take part in the central pattern generation circuits. A scheme in which chromatophore motoneurons act as readouts for wave and static displays is more parsimonious. We thus hypothesize the existence of dedicated and premotor wave-pattern-generating circuits, upstream of the chromatophore motoneurons. Rhythmic bursting neurons in the *Octopus vulgaris* posterior chromatophore lobes have been observed in intracellular recordings in vivo [16] (with a period of 2–3 s, which is longer than the duration of passing clouds reported for octopuses [approximately 1 s] but is possibly explained by experimental cooling of the preparation).

At least three different general classes of circuits could generate periodic traveling waves [3, 4] (see also Figure S2). The first consists of an oscillator connected to an array of common targets (e.g., neurons or muscles). If delays between the oscillator and its targets increase systematically along the array, the appearance of a traveling wave will be created. The connection between the driver oscillator and the responders need not necessarily be direct. It can result from a signal propagating through a network of intrinsically excitable elements (e.g., neurons [17], smooth muscles [18], astrocytes [19], and possibly denervated chromatophores participating in wandering clouds [1, 14]) in a feedforward fashion, in which every element excites a few of its nearest neighbors further down the chain. However, whatever the origin of the delay, the spatial wavelength of the pattern in such a design increases

proportionally with the period of the driving oscillator. Because the wavelength of the *Metasepia* wave display is independent of the period, we can rule out all realizations of circuits based on this principle.

A second class of circuits capable of generating traveling waves involves an array of weakly coupled oscillators that can phase lock their activity [20]. If there is asymmetric connectivity [21] or a uniform gradient of intrinsic oscillator frequencies along the array [22], the phase delay between neighboring oscillators will be constant, and a periodic wave will travel across the system in one direction and with a period-independent wavelength. This design is proposed, for example, to underlie swimming body movements in fish [23] and tadpoles [24] and crawling locomotion in insect larvae [25]. It is also fully compatible with all the observed properties of the *Metasepia* wave display. If it is indeed the class of circuits used to drive chromatophore traveling waves in cephalopods, it points toward the locomotor system (more specifically, the network used to control wave-like undulations of the cephalopod fin during swimming; indeed, chromatophore and fin motion motoneurons lie intermingled in the fin lobes of *S. officinalis* [26]) as a possible evolutionary ancestor of our hypothesized premotor pattern-generating circuit [27].

A third class relies on periodic circuit topology [4]. In its simplest form, an array of neurons with feedforward and closed (circular) connectivity can, if excited appropriately and connected to a linearly arranged readout (e.g., the chromatophore array), generate waves identical to those produced by the second class. Whereas the period of the traveling wave is controlled by modulations in oscillator frequency in a system of the second class, it is the propagation velocity along the ring that allows control over the period in the third.

Because circuits of the second and third type can produce equivalent outputs, we cannot choose between them based on behavioral evidence alone. If, however, some further experimentation could provide support for one circuit over the other, our behavioral findings would provide constraints to pin down the details of its biophysical implementation. For example, if a circuit of class 2 was established, our finding of a period-independent duty cycle would point toward multicellular oscillators. Oscillators created through the actions of voltage-activated currents within a single cell typically have a period-dependent duty cycle (consider for example the cardiac pacemaker or neuronal action potentials) [28, 29]. By contrast, a period-independent duty cycle is easy to establish in an oscillator composed of two mutually inhibiting half-centers [30]. In the unperturbed state, one can see by symmetry that each half-center will be active for roughly half the duty cycle, whatever the period may be, and selective input into one half-center can be used to modulate the duty cycle around the mean, default value.

Upon naive inspection, the finding of four different regions of wave propagation, each with its distinct propagation direction, might suggest the presence of four distinct central control systems. However, the observed synchrony (across sides and across regions on one side) suggests that all the wave patterns may be generated by a single central control system mapped onto the body via region-specific axonal projection patterns [31] in four different ways on each side. Because we have argued that chromatophores (or chromatophore motoneurons) act as readouts of the premotor wave-pattern-generating circuit, the presence of selective spatial gating can be reconciled with the notion of a single central controller by postulating a region-selective presynaptic gating

mechanism [32]. However, behavioral experiments cannot definitively rule out the presence of multiple control systems because coupling between multiple control systems could establish their mutual synchrony [22].

References

1. Messenger, J.B. (2001). Cephalopod chromatophores: neurobiology and natural history. Biol. Rev. Camb. Philos. Soc. *76*, 473–528.
2. Hanlon, R.T., Chiao, C.C., Mäthger, L.M., Barbosa, A., Buresch, K.C., and Chubb, C. (2009). Cephalopod dynamic camouflage: bridging the continuum between background matching and disruptive coloration. Philos. Trans. R. Soc. Lond. B Biol. Sci. *364*, 429–437.
3. Ermentrout, G.B., and Kleinfeld, D. (2001). Traveling electrical waves in cortex: insights from phase dynamics and speculation on a computational role. Neuron *29*, 33–44.
4. Xie, X., Hahnloser, R.H.R., and Seung, H.S. (2002). Double-ring network model of the head-direction system. Phys. Rev. E Stat. Nonlin. Soft Matter Phys. *66*, 041902.
5. Mather, J., and Mather, D.L. (2004). Apparent movement in a visual display: the 'passing cloud' of *Octopus cyanea* (Mollusca: Cephalopoda). J. Zool. (Lond.) *263*, 89–94.
6. Hanlon, R.T., and Messenger, J. (1988). Adaptive coloration in young cuttlefish (*Sepia officinalis* L.): the morphology and development of body patterns and their relation to behaviour. Philos. Trans. R. Soc. Lond. B Biol. Sci. *320*, 437–487.
7. Adamo, S.A., Ehgoetz, K., Sangster, C., and Whitehorne, I. (2006). Signaling to the enemy? Body pattern expression and its response to external cues during hunting in the cuttlefish *Sepia officinalis* (Cephalopoda). Biol. Bull. *210*, 192–200.
8. Norman, M.D., Finn, J., and Tregenza, T. (1999). Female impersonation as an alternative reproductive strategy in giant cuttlefish. Philos. Trans. R. Soc. Lond. B Biol. Sci. *266*, 1347–1349.
9. Roper, C.F.E., and Hochberg, F.G. (1988). Behavior and systematics of cephalopods from Lizard Island, Australia, based on color and body patterns. Malacologia *29*, 153–193.
10. Froesch-Gaetzi, V., and Froesch, D. (1977). Evidence that chromatophores of cephalopods are linked by their muscles. Experientia *33*, 1448–1450.
11. Reed, C.M. (1995). Dye coupling in the muscles controlling squid chromatophore expansion. J. Exp. Biol. *198*, 2631–2634.
12. Sanders, G.D., and Young, J.Z. (1974). Reappearance of specific color patterns after nerve regeneration in octopus. Philos. Trans. R. Soc. Lond. B Biol. Sci. *186*, 1–11.
13. Hoffmann, F.B. (1907). Gibt es in der Muskulatur der Mollusken periphere kontinuierlich leitende Nervennetze bei Abwesenheit von Ganglienzellen? I. Untersuchungen an Cephalopoden. Pflügers Arch. Ges. Physiol. *118*, 375–413.
14. Packard, A. (1995). Organization of cephalopod chromatophore systems: a neuromuscular image-generator. In Cephalopod Neurobiology, J. Abbott, R. Williamson, and L. Maddock, eds. (Oxford: Oxford University Press), pp. 415–429.
15. Nixon, M., and Young, J.Z. (2003). The Brains and Lives of Cephalopods, First Edition (Oxford: Oxford University Press).
16. Miyan, J.A., and Messenger, J.B. (1995). Intracellular recordings from the chromatophore lobes of octopus. In Cephalopod Neurobiology, J. Abbott, R. Williamson, and L. Maddock, eds. (Oxford: Oxford University Press), pp. 415–429.
17. Wong, R.O. (1999). Retinal waves and visual system development. Annu. Rev. Neurosci. *22*, 29–47.
18. Karaki, H., Ozaki, H., Hori, M., Mitsui-Saito, M., Amano, K., Harada, K., Miyamoto, S., Nakazawa, H., Won, K.J., and Sato, K. (1997). Calcium movements, distribution, and functions in smooth muscle. Pharmacol. Rev. *49*, 157–230.
19. Scemes, E., and Giaume, C. (2006). Astrocyte calcium waves: what they are and what they do. Glia *54*, 716–725.
20. Wallén, P., and Williams, T.L. (1984). Fictive locomotion in the lamprey spinal cord in vitro compared with swimming in the intact and spinal animal. J. Physiol. *347*, 225–239.
21. Hagevik, A., and McClellan, A.D. (1994). Coupling of spinal locomotor networks in larval lamprey revealed by receptor blockers for inhibitory amino acids: neurophysiology and computer modeling. J. Neurophysiol. *72*, 1810–1829.
22. Kopell, N., and Ermentrout, B. (1986). Symmetry and phaselocking in chains of weakly coupled oscillators. Commun. Pure Appl. Math. *39*, 623–660.
23. Grillner, S. (1985). Neurobiological bases of rhythmic motor acts in vertebrates. Science *228*, 143–149.
24. Roberts, A., Soffe, S.R., Wolf, E.S., Yoshida, M., and Zhao, F.Y. (1998). Central circuits controlling locomotion in young frog tadpoles. Ann. N Y Acad. Sci. *860*, 19–34.
25. Pulver, S.R., and Griffith, L.C. (2010). Spike integration and cellular memory in a rhythmic network from Na+/K+ pump current dynamics. Nat. Neurosci. *13*, 53–59.
26. Gaston, M.R., and Tublitz, N.J. (2006). Central distribution and three-dimensional arrangement of fin chromatophore motoneurons in the cuttlefish *Sepia officinalis*. Invert. Neurosci. *6*, 81–93.
27. Striedter, G.F. (2004). Principles of Brain Evolution (Sunderland: Sinauer Associates).
28. Bazett, H.C. (1920). An analysis of the time-relations of electrocardiograms. Heart *7*, 353–370.
29. Strogatz, S. (2001). Nonlinear Dynamics and Chaos (Boulder: Westview Press).
30. Matsuoka, K. (1987). Mechanisms of frequency and pattern control in the neural rhythm generators. Biol. Cybern. *56*, 345–353.
31. Sosulski, D.L., Bloom, M.L., Cutforth, T., Axel, R., and Datta, S.R. (2011). Distinct representations of olfactory information in different cortical centres. Nature *472*, 213–216.
32. MacDermott, A.B., Role, L.W., and Siegelbaum, S.A. (1999). Presynaptic ionotropic receptors and the control of transmitter release. Annu. Rev. Neurosci. *22*, 443–485.